Thermochimica Acta 623 (2016) 1–8

Contents lists available at ScienceDirect

Thermochimica Acta

journal homepage: www.elsevier.com/locate/tca

Spherulitic growth and crystallization kinetics in PHB/DGEBA blends

Sebastián Tognana[a,b,*], Walter Salgueiro[a,b], Leonel Silva[c]

[a] IFIMAT, Facultad de Ciencias Exactas, CIFICEN CONICET, UNCPBA, Pinto 399, 7000 Tandil, Argentina
[b] Comisión de Investigaciones Científicas de la Provincia de Buenos Aires, Calle 526 entre 10 y 11, 1900 La Plata, Argentina
[c] INTEMA—CONICET, Universidad Nacional de Mar del Plata, Av. Juan B Justo 4302, 7608 Mar del Plata, Argentina

ARTICLE INFO

Article history:
Received 4 August 2015
Received in revised form 5 November 2015
Accepted 6 November 2015
Available online 10 November 2015

Keywords:
Crystallization
Blends
Poly(3-hydroxybutyrate)
Epoxy resin
Differential scanning calorimetry (DSC)

ABSTRACT

A study of spherulitic growth in PHB and PHB/DGEBA (poly(3-hydroxybutyrate)/diglycidyl ether of bisphenol A) blends with PHB/DGEBA weight ratios of 100/0, 90/10, 80/20, 70/30 and 60/40 crystallized at temperatures in the range of 45–110 °C is carried out. The spherulitic growth rates at the crystallization temperatures are studied by optical microscopy. Differential scanning calorimetry is used to study the same isothermal process to fit the results by means of the Avrami theory to determine the characteristic parameters of the process. The obtained characteristic parameters are compared to the spherulitic growth rates that are determined by optical microscopy. The observed differences are discussed considering the process of nucleation. An increase in the secondary crystallization process is observed with increasing crystallization temperature and DGEBA content in the blend. Changes in the crystallization associated with an increase in the rigid amorphous fraction (RAF) mobility are discussed.

1. Introduction

The blending of polymers and the study of the physical processes involved in the development of blends with specific characteristics are the goals of research pursued at the present, for instance, to improve the characteristics of environmentally sustainable materials. The importance of this type of study arises because some environmentally sustainable blend constituents have demonstrated limitations from the perspective of practical applications, such as a deficient or limited mechanical response or other properties that compromise their response in engineering applications. The improvement of the specific properties of a polymer that exhibits some type of limitation can be achieved by blending it with others polymers that are commonly used because of their very good properties that have been recognized from extensive applications. Biodegradable polymers obtained from natural resources are used in blends, but generally have the disadvantage of a high degree of crystallinity [1,2]. One such natural polymer is poly(3-hydroxybutirate) (PHB); thus, efforts have been made to reduce the high brittleness of this material attributed to its high crystallinity [3–5]. Furthermore PHB as component of polymer blends, is the subject of study because its biodegradability suggests a potential use in replacing conventional polymers to improve the environmental sustainability of the blends produced. Epoxy is a widely used thermoset polymer; however, blending with semicrystalline polymers, such as PHB, has been scarcely addressed in the literature [6,7]. Furthermore, the complexity and richness of the process of crystallization in PHB and PHB blends have distinguished this polymer as a model with important features that should be studied from an academic perspective as well as toward applications.

Many studies of the crystallization kinetics of homopolymers are based on the measurement of the spherulitic growth rates; see, for instance [4], and the references therein. The theoretical framework is usually referred as the Lauritzen–Hoffman theory [8,9], which describes the linear growth rate G_e of spherulites as:

$$G_e = \frac{dR_e}{dt} = G_0 \exp\left[\frac{-U^*}{R(T_c - T_\infty)}\right] \exp\left(\frac{-K_g}{fT_c\Delta T}\right) \quad (1)$$

where, R_e is the spherulite radius, G_0 is the pre-exponential factor and contains terms that are essentially temperature independent, U^* is the activation energy for transport of crystallizable segments to the crystallization front, T_∞ is the temperature below which such motions cease, T_c is the crystallization temperature, R is a universal gas constant, $\Delta T = T_m^0 - T_c$ is the degree of undercooling, T_m^0 is the equilibrium melting point, and f is a factor that accounts for variation in the enthalpy of fusion with temperature and is given by

* Corresponding author at: IFIMAT, Facultad de Ciencias Exactas, UNCPBA, Pinto 399, Tandil, Argentina. Tel.: +54 2494385670.
E-mail address: stognana@exa.unicen.edu.ar (S. Tognana).

http://dx.doi.org/10.1016/j.tca.2015.11.009
0040-6031/

$f = 2T_c/\left(T_m^0 - T_c\right)$. The nucleation constant K_g can be expressed as [8]:

$$K_g = \frac{mb_0\sigma\sigma_e T_m^0}{\Delta h_f k} \quad (2)$$

where, σ and σ_e are the lateral and end-surface free energies, respectively, of the growing crystals; b_0 is the molecular thickness; Δh_f is the heat of fusion; and k is the Boltzman constant. The value of m depends on the regime of crystallization. At high temperatures (low undercoolings), each surface nucleation occurrence leads to the rapid competition of the growth strip prior to the next nucleation event [4].

The lateral free energy can be obtained using the empirical equation:

$$\sigma = \alpha\Delta h_f(a_0 b_0)^{1/2} \quad (3)$$

where, α is an empirical constant equal to 0.25 for high melting polyesters [4] and a_0 is the molecular width equal to 0.66 nm for PHB.

However, for blends containing a fraction ϕ of crystallizable component (PHB in this case), a modification of Eq. (1) is usually used to consider the non-crystallizable component [10].

$$G = \phi G_0 \exp\left(\frac{-U^*}{R(T - T_\infty)}\right)\exp\left(\frac{-K_g}{fT\Delta T} + \frac{2\sigma T_m^0 \ln\ \phi}{fb_0\Delta H\,\Delta T}\right) \quad (4)$$

Eq. (4) can be rewritten in the form:

$$\ln\ G + \frac{U^*}{R(T - T_\infty)} - \frac{2\sigma T_m^0 \ln\ \phi}{fb_0\Delta H\Delta T} = \ln(\phi G_0) - \frac{K_g}{fT\Delta T} \quad (5)$$

If the crystallization occurs in a blend containing a non-crystallizable component, this component is rejected from the lamellae. This rejection can be produced toward the interlamellar region, i.e., near the crystalline region, or toward the interfibrillar or interspherulitic regions. The location of the non-crystallizable component depends on the interplay between a force that tends to pull the molecules out of interlamellar regions and a force that attempts to keep the molecules joined [11]. The first is a product of the lower conformational entropy due to the lower dimensionality of the interlamellar region, and the second is due to favorable interactions between the non-crystallizable component and the amorphous phase.

The temperature crystallization range is located between the glass transition temperature T_g and the equilibrium melting temperature T_m^0 [12]. When T_c is near T_g, the kinetics of crystallization will be controlled by the chain mobility; therefore, G increases as T_c increases. Conversely, if T_c is near T_m^0, the rate of crystallization is conduced by the thermodynamic regime. The interaction between the two processes produces a maximum in G at a temperature T_k between T_g and T_m^0. An empiric relationship between these temperatures was reported as [13]:

$$T_k \approx 0.5\left(T_m^0 + T_g\right) \quad (6)$$

On the other hand, the kinetics of overall crystallization can be studied using different techniques, particularly calorimetry. If it is assumed that the crystallinity is directly proportional to the heat during the isothermal crystallization, the relative crystallinity can be obtained from:

$$X(t) = \frac{H(t)}{H_0} \quad (7)$$

where, $H(t)$ is the heat released at time t and H_0 is the total heat.

$X(t)$ can be modeled using the well-known Avrami equation (see e.g., reference [14]):

$$1 - X(t) = \exp(-k_A t^n) \quad (8)$$

where, k_A and n are the rate of crystallization and the Avrami index, respectively. In this work, we assumed that the volume changes do not appreciably affect the crystallization growth rate.

A modification of this equation considers an induction time (t_0) before which crystallization starts replacing t by $t - t_0$. Then, Eq. (8) becomes:

$$1 - X(t) = \exp(-k_A(t - t_0)^n) \quad (9)$$

The induction time (or incubation period of crystallization) can be interpreted as a measure of the time required for statistic processes to produce a nucleus of sufficient size for growth. The determination of t_0 is not easy because it depends in great measure on the device used and has a strong influence on the analysis of thermograms; in this sense, different analytical methods have been used [15].

In the field of research of blends containing biodegradable materials, such as PHB, the authors of the present work have developed studies of miscibility [16], crystallization [17] and segregation during crystallization [18] in blends of PHB/DGEBA. DGEBA is a common monomer that is used in epoxy systems, and the study of PHB/DGEBA blends is a first step to prepare PHB/epoxy blends. The present work adds new information to the study of PHB/DGEBA blends by reporting the results of the kinetics of the crystallization process, that is, the spherulitic growth rates, nucleation process and secondary crystallization process. The analysis of the results combined with the reported results allows the parameters of crystallization to be determined in the framework of the Hoffman–Lauritzen theory. However, some findings are raised as points of discussion.

2. Experimental

PHB powder with the trade name Biocycle® was supplied by Industrial (Brazil). The epoxy monomer diglycidyl ether of bisphenol A (DGEBA) was supplied by Hunstman (Araldite MY 790). Blend samples with PHB/DGEBA weight ratios of 100/0, 90/10, 80/20, 70/30 and 60/40 were studied.

To determine the spherulitic growth rates, optical microscopy was used with a PME OLYMPUS TOKYO microscope with polarizer and a CCD camera to record the micrographs. A specially designed hot plate was used to maintain the temperature at the selected crystallization temperature. The samples were melted at 180 °C and kept at a constant temperature for 120 s in an exterior oven. Then, a small amount of sample was quickly poured between two plates that were previously heated to the selected crystallization temperature (T_c) between 45 °C and 100 °C. The temperature was maintained until the spherulite growth stopped, and then, the micrographs were regularly collected. From the micrographs that were obtained, the radii of the spherulites were determined using image processing software.

The isothermic crystallization was studied by differential scanning calorimetry (DSC) using a Q20 by TA Instruments. The calorimeter was calibrated using indium as a reference material. The measurements were taken under an argon atmosphere with a constant flux of 50 mL/min in a range of T_c between 45 °C and 100 °C. Samples with a mass between 6 and 12 mg were heated in aluminum pans at a heating rate of 10 °C/min from room temperature to 190 °C and were thermostabilized for 120 s at this temperature. Then, they were submitted to cooling at 65 °C/min until reaching T_c and were thermostabilized at T_c until the completion of the crystallization process.

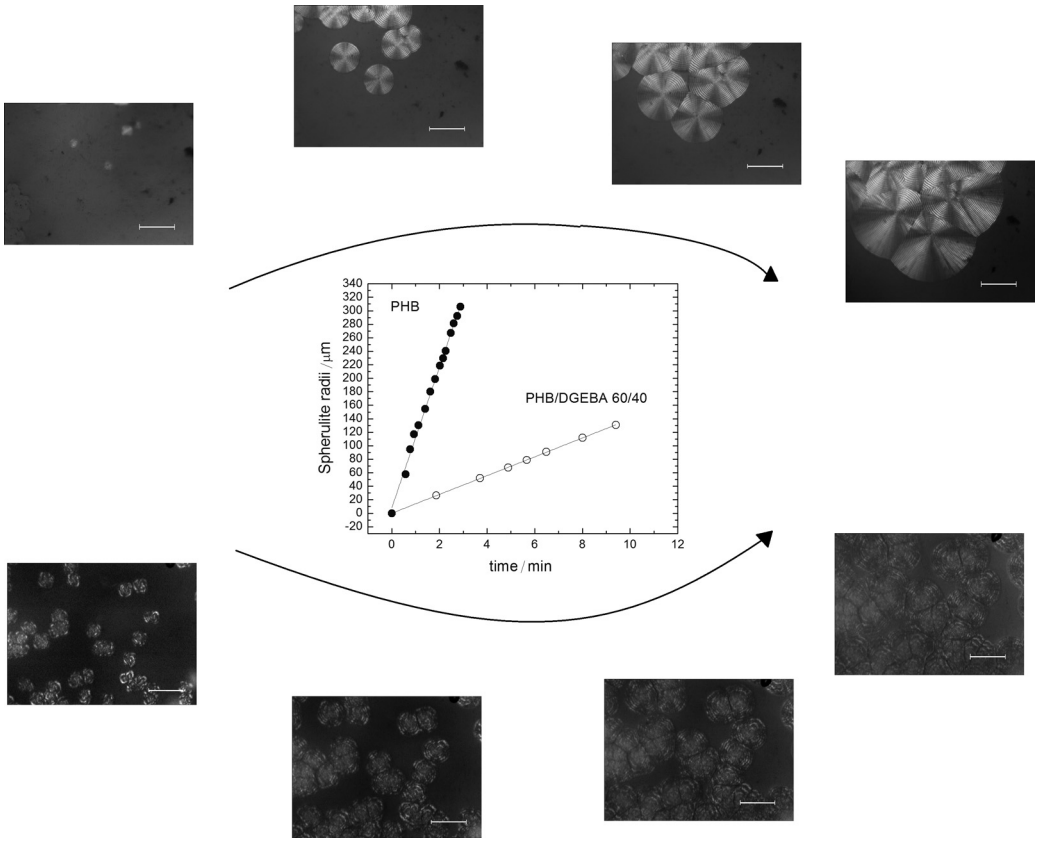

Fig. 1. Micrographs of pure PHB at 55 °C (at the top) and the PHB/DGEBA 60/40 blend at 80 °C (same magnification, bar = 100 μm). Spherulite radii as a function of time for PHB and PHB/DGEBA 60/40 crystallized at 80 °C.

3. Results and discussion

3.1. Spherulitic growth

In Fig. 1, some micrographs of spherulites in PHB and blends are shown as examples. As observed, the PHB crystallizes, forming banded spherulites.

The spherulite radius was determined at different times using the micrographs. In the graph of Fig. 1, the spherulite radius as a function of time for T_c = 80 °C is depicted as a representative example. From the analysis of all of the measurements, it can be concluded that the results of R_e as a function of time can be well fit by linear regression (r^2 = 0.99). The authors have reported that there is interlamellar segregation for a DGEBA content lower than 30% in PHB/DGEBA blend, which does not depend on the crystallization temperature [16,17]. For a DGEBA content higher than 30%, the segregation can be interfibrillar or interspherulitic. The interspherulitic segregation can produce changes in the spherulitic growth because the DGEBA is segregated toward the front of growth, changing the composition in this region. However, no variation of spherulitic growth as a function of time was observed and interspherulitic segregation would not develop.

From the slope of linear regression shown in Fig. 1, the spherulite growth rates (G) were obtained for pure PHB and blends PHB/DGEBA 90/10, 80/20, 70/30 and 60/40 at the different crystallization temperatures studied. No distinction of notation is made between G_e (PHB) and G (blends); only G is used further in this work. The values of G obtained are presented in Fig. 2a as a function of T_c.

As can be observed in Fig. 2a, G shows a maximum at $T_c \approx 87$ °C for pure PHB. The temperature at the maximum growth rate, T_k, decreases with the content of PHB in the blend. In the literature, T_k for PHB and blends is reported to be near 90 °C [4,19–21]. Moreover,

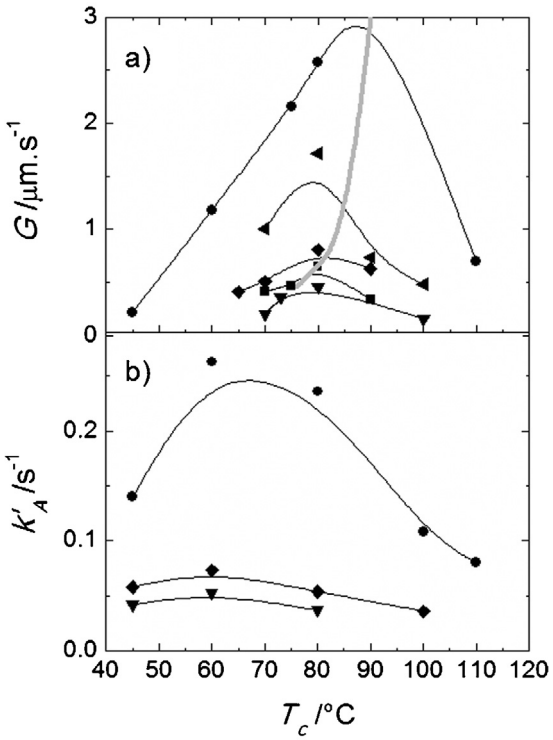

Fig. 2. (a) G as a function of T_c for PHB (•) and blends with ratios of PHB/DGEBA of 90/10 (◄), 80/20 (♦), 70/30 (■), 60/40 (▼). The gray line connecting approximately the maximum of G is the empirical relationship given by Eq. (6). (b) k'_A as a function of T_c for PHB (•) and blends with ratios of PHB/DGEBA of 80/20 (♦) and 60/40 (▼) (see text). The lines connecting experimental points are only visual guides.

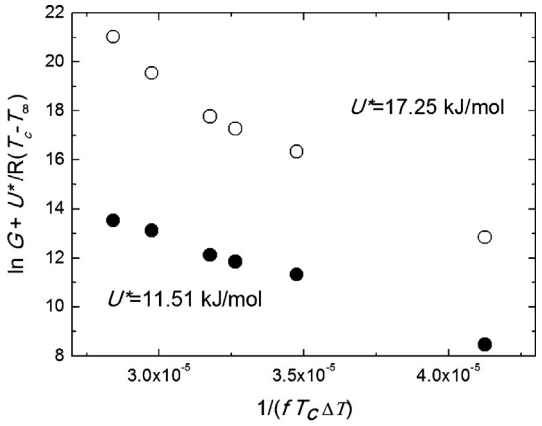

Fig. 3. Left side of Eq. (5) for pure PHB ($\phi = 1$) as a function of $1/fT_c\Delta T$ for different values of U^*.

G also decreases when the PHB content decreases. Using Eq. (6) and the values of T_m^0 and T_g reported by the authors, the values of T_k were estimated [16]. A gray line connecting these values is plotted as a visual guide in Fig. 2a along with the experimental values of G. As observed, the estimation of maximum G agrees approximately with the experimental results.

A diminution of G with the aggregate of the non-crystallizable component has been observed in PHB/poly(vinylidene chloride-co-acrylonitrile) blends [22]; however, in that case, the T_g of the non-crystallizable component is higher than the T_g of PHB. Similarly, for PHB/poly(*p*-vinphenol), the depression in G when the content of the non-crystallizable component increases was attributed to changes in the fluidity due to an increase in T_g [23]. In the case of PHB/DGEBA, this explanation cannot be used because the T_g of the blends PHB/DGEBA decreases with the non-crystallizable content, as was shown in a previous work [16]. It is worth mentioning that the equilibrium melting points for the blends were also reported in a previous work, where T_g decreases from 2.6 °C in pure PHB to −10 °C in PHB/DGEBA 50/50 and the equilibrium melting point decreases from 179 °C to 155 °C in the same samples.

In PHB/DGEBA blends, the authors recently reported a value of −0.86 for the interaction parameter in the molten state [16], which ensures a force of interaction between DGEBA and amorphous PHB. On the other hand, DGEBA is a small molecule compared to other polymers used as components in blends with PHB. Thus, it is expected to have a weak entropic force.

The spherulitic growth rates at temperature T_c in a homopolymer can be analyzed using Eq. (1). From Eqs. (1) and (5), the values of K_g and G_0 can be estimated by plotting the left side of Eq. (5) as a function of $1/fT_c\Delta T$.

It is difficult to calculate K_g and σ_e because the values of U^* and T_∞ are unknown. The usual procedure is to choose these parameters such that they provide the best fit in the plot of the left side of Eq. (5) versus $1/fT_c\Delta T$. Values between 6.28 kJ/mol and 17.25 kJ/mol have been used in the literature [24], the first, assumed as an universal value, and the second corresponds to the William–Landel–Ferry theory (WLF) [25]. However, this procedure could hide an eventual variation of σ_e with the crystallization temperature. For example, in Fig. 3, the mentioned plot is presented for two values of U^*: 11.51 kJ/mol and 17.25 kJ/mol, the first of which is used by Pearce et al. Whereas the first value produces more linear behavior, the second exhibits a change in slope at the crystallization temperature of approximately 80 °C. Then, a linear fit in the second case produces an "average" value of the slope. This change in the slope could, however, have significance if it is considered that a rigid amorphous fraction (RAF) exists between the crystalline and mobile amorphous fraction (MAF). It is known that this region

Table 1
K_g and G_0 obtained from G versus T_c curves, σ_e calculated from Eq. (2) and q for pure PHB and PHB/DGEBA blends.

Sample	K_g ($\times 10^5$ K^2)	G_0 (m/s)	σ_e ($\times 10^{-3}$ J/m^2)	q (kJ/mol)
100/0	5.9 ± 0.4	9.5 ± 0.5 × 10^9	50.5 ± 3.6	23.4 ± 1.6
90/10	5.7 ± 0.6	3.0 ± 0.3 × 10^9	48.9 ± 5.3	22.6 ± 2.5
80/20	4.2 ± 0.2	2.3 ± 0.9 × 10^7	36.2 ± 1.8	16.7 ± 0.8
70/30	3.9 ± 0.4	1.5 ± 0.2 × 10^7	34.0 ± 3.6	15.5 ± 1.6
60/40	2.4 ± 0.3	1.8 ± 0.1 × 10^5	22.1 ± 7.1	10.1 ± 3.0

vitrifies when the crystallization is produced at temperatures lower than approximately 70 °C. The hypothesis being considered in this work is that the surface free energy feels the influence of the RAF and the state of the RAF, vitrified or not. For temperatures lower than 70 °C, the region around the crystals is vitrified and the surface free energy is higher than that for the case of temperatures higher than 70 °C, at which the RAF is not vitrified. If a different T_∞ of 203 °C is used, which was obtained for Pearce et al. [4], a similar behavior is observed; obviously, different values for the slope are obtained. However, at this point, it is difficult to determine whether the change in slope in Fig. 3 is due to a change in σ_e or an over or underestimated value of U^*. Therefore, henceforth, the value of a single slope will be analyzed. The values of U^* and T_∞ were assumed to correspond to the WLF theory: $U^* = 17.25$ kJ/mol, $T_\infty = T_g - 51.6$ K [25] and $b_0 = 0.58$ nm [4]. In this case, the values of K_g are presented in Table 1 for PHB and the blends studied. The values of ϕ were calculated from volume additivity using density values of 1.177 g cm^{-3} for amorphous PHB [19] and 1.200 g cm^{-3} for DGEBA [26].

From Eq. (2), the values of σ_e were calculated for PHB and the PHB/DGEBA blends considering that for the temperatures used in this work, crystallization occurs in regime III, which corresponds to $n = 4$ [4,19]. The value of σ_e for pure PHB (see Table 1) is within the range obtained in the literature: Pearce et al. [4] obtained 46×10^{-3} J/m^2, Xing et al. [23] obtained 42.74×10^{-3} J/m^2 and Zhang et al. [27] obtained 58.7×10^{-3} J/m^2. On the other hand, Barham et al. [19] obtained a higher value for σ_e, 94×10^{-3} J/m^2.

For the blends, σ_e decreases with increasing DGEBA content. A diminution of σ_e has been observed in blends of PHB/poly(epichlorohydrin-co-ethylene oxide) [27] and PHB/P(VAc-co-VA9) [23]. Usually, it is assumed that the work of chain folding $q = 2b_0a_0\sigma_e$ is the parameter most related to chain structure and chain stiffness [4,23,27]; this is shown in column 5 of Table 1. A reduction of q is observed, indicating more flexible chains of PHB in the blends.

In a recent work, some of the authors calculated the value of $\gamma\sigma_e$ from the value of the dimension of the crystalline phase L [18], assuming an ideal two-phase structure at a crystallization temperature of 100 °C using Eq. (10):

$$L = \gamma L_g = \gamma \left(\frac{2\sigma_e T_m^0}{\Delta h_f \left(T_m^0 - T_c \right)} + \delta \right) \tag{10}$$

In Eq. (10), γ is the ratio of initial to final lamellar dimension due to thickness and δ is a term that gives stability to the crystal. In the mentioned work, δ was assumed to be zero and the result for $\gamma\sigma_e$ was 0.079 J/m^2. Using the value of σ_e shown in Table 1, a value of 1.56 can be calculated for γ. This value is lower than the usually expected value of 2, but there is scarce information in the literature about this parameter in PHB. γ can be determined from the inverse of the slope in a plot of T_m versus T_c or a Hoffman–Weeks plot. In fact, the T_m dependency on T_c can be written as:

$$T_m = T_m^0 \left(1 - \frac{1}{\gamma} \right) + \frac{T_c}{\gamma} \tag{11}$$

From this procedure, Dubini Paglia et al. gave an approximate value of 3.33 for PHB [28]. In many other works, the

Hoffman–Weeks plot was shown, but the value of the slope was not reported; therefore, we estimated them from a visual analysis of the figures; in general, we found that the γ values were in the range ≈3–6. In fact, we recently reported a Hoffman–Weeks plot for PHB [16], and the observed slope gave a value of ≈5. A value near 5 would indicate an important thickening of crystals. Heo et al. [29] studied the crystalline dimension during crystallization in PHB at 125 °C, 135 °C and 145 °C but observed almost no thickening for crystallization times higher than ≈100 s. Guo et al. reported that the crystalline dimension was a function of time for crystallization at 120 °C and showed an increase until 100 s [30]. They analyzed the results using a crystallization model that considered intermediate states; however, the results showed that the thickening in the entire crystallization was significantly lower than 2. Moreover, there are arguments to support a value of γ near 1, and the value of 1.56 determined as explained above seems to be a realistic value.

The process mentioned in the previous paragraph leads to a question about the higher values of the slope in the Hoffman–Weeks plot. One possible explanation comes from revisiting Eq. (10), as accomplished by Rim et al. [31]. In Eq. (10), a value of δ equal to zero is assumed; however, if this parameter is different from zero, a nonlinear behavior can be expected and the slope obtained would be an apparent value. Thickening during heating in the calorimetric measurement also could influence the value of γ.

The authors also reported the values of $\gamma\sigma_e$ for blends PHB/DGEBA 90/10 = 0.068 J/m^2 and PHB/DGEBA 70/30 = 0.061 J/m^2. If the values of σ_e presented in Table 1 are used to calculate γ, the values of 1.39 and 1.79 can be obtained for blends 90/10 and 70/30, respectively; therefore, it can be concluded that γ presents values lower than 2 with no strong variation in DGEBA content for the proportions studied.

The estimated values of G_0 are also presented in Table 1. A decrease of G_0 is observed when the DGEBA content increases. The G_0 diminution explains the decrease of G when the DGEBA content increases.

Whereas Pizzoli et al. observed no variation of G_0 for blends PHB/DPB [32], Pearce et al. [4] reported a diminution of G_0 in isotactic and atactic PHB blends, indicating that the pre-exponential factor in Eq. (1) is strongly affected by the aggregation of the non-crystallizable component, underscoring the importance of the diffusion of non-crystallizable and crystallizable components. Alfonso et al. [33] proposed equations to consider the diffusion of the non-crystallizable component from the growth front, but they require self-diffusion coefficients to be applied. This treatment is consistent with the findings of Keith et al., who suggested that the location of the non-crystallizable component depends on segregation distance, which is the ratio between the diffusion rate D of the amorphous molecules and the crystal growth rate [34]. If D is lower than G, the non-crystallizable component is trapped in a position close to that occupied before solidification [11]. Previous works performed by the authors showed that the segregation is interlamellar for a DGEBA content lower than 30% and interspherulitic or interfibrillar for a DGEBA content higher than 30%. Thus, the results of G_0 are qualitatively in agreement with the mentioned conclusion because, assuming a weak dependence of D on the DGEBA content as a first approximation, a higher segregation distance is produced in the blends with a lower G value.

3.2. DSC results

DSC results were obtained in isothermal conditions for PHB and blends PHB/DGEBA 90/10, PHB/DGEBA 80/20 and PHB/DGEBA 70/30 for different crystallization temperatures. It can be observed that the initial heat flux is not zero in some cases because of the limitations of the calorimeters, which usually have difficulty generating a higher cooling rate. Obviously, during the time of cooling and during the time that the device reaches the stabilization temperature, no isothermal crystallization can be produced. It is well known that difficulties exist in this type of analysis, and these are discussed in the literature; for instance, Lorenzo et al. [15] recommended that in crystalline polymers, the cooling rate would be higher than 60 °C/min. In this work, the equipment used has allowed a cooling rate of ≈65 °C/min. The data analysis procedure followed in this work was to subtract the thermogram corresponding to the pan without the sample from the thermogram with the sample, with the aim of eliminating the response of the device due to cooling. In Fig. 4, the results obtained following that procedure are shown. In general, a clear peak was obtained after the mentioned procedure; however, for T_c = 60 °C and specifically for T_c = 80 °C, the subtraction of the thermogram corresponding to the pan do not result in a shift of the curve until the zero line, and the onset of the peak is still high. Thus, to consider the entire contribution of the pan, a new subtraction of a straight baseline was performed. The same procedure was performed for the PHB/DGEBA blends 90/10, 80/20 and 70/30. For the PHB/DGEBA 60/40 blend, the thermograms obtained did not allow for the analysis described because the heat flow obtained was not sufficient. In Fig. 4b, it is observed that for the crystallization of PHB/DGEBA at temperatures of 80 °C and 100 °C (temperatures selected as an example), the peaks are broader than for 60 °C.

The heat flow can be derived from Eq. (9):

$$\frac{dH}{dt}(t) = \exp(-k_A(t-t_0)^n)k_A n(t-t_0)^{n-1}H_0 \quad (12)$$

This equation can be used to directly fit the experimental thermogram in the first part of the curve, taking as free parameters k_A, t_0, n and H_0. The advantage of this procedure with respect to the usual one (calculate $H(t)$ by integrating the heat flow and then use the Avrami equation as a theoretical function for fitting) resides in the difficulties that arise for an estimation of H_0 because some heat is lost during cooling, and therefore the area under the curve cannot exactly represent a measure of H_0. Moreover, in this work, t_0 was used as a free parameter to fit the experimental results using Eq. (12). Furthermore, considering that the Avrami equation only describes the primary crystallization, the fitting was performed until the fraction of crystalline reached 50%.

The results of fitting for different T_c and compositions are presented following ideas reported in the literature by calculating the parameter $k'_A = k_A^{1/n}$, which is a normalized rate [35]. The results of n are presented in Table 2, and selected results (for clarity in the presentation) of k'_A for PHB and blends with ratios PHB/DGEBA, 80/20 and 60/40 are depicted in Fig. 2b together with the plot of G as a function of T_c. According to the literature, k'_A shows a dependency on T_c similar to that observed for G. Effectively, a similar equation to Eq. (1) can be used to describe k'_A as a function of T_c.

$$k'_A = k'_{A0}\exp\left[\frac{-U^*}{R(T_c - T_\infty)}\right]\exp\left(\frac{-K_g}{fT_c\Delta T}\right) \quad (13)$$

where, k'_{A0} is a pre-exponential factor, and the other parameters are as defined before.

Fig. 2b shows that the maximum of k'_A as a function of T_c is shifted to lower temperatures with respect to the plot of G at a value of approximately 20 °C. Then, the estimation of parameter K_g from k'_A will be inaccurate. In fact, an estimation of K_g for pure PHB using U^* and T_∞ from the WLF theory indicates a value of K_g = 7.2 (±1.1) × 10^5 K^2, which is 22% higher than that obtained from the experimental G results ($K_g = 5.9 \times 10^5$ K^2). This is in agreement with Celli et al. [36], who concluded that although K_g, and consequently σ_e, could be calculated from G or from the parameters of the Avrami equation, significant differences can be observed between the calculated values. Moreover, the authors reported that the values calculated from Avrami parameters are higher by 15–50% with respect to those calculated from G because they are more exact.

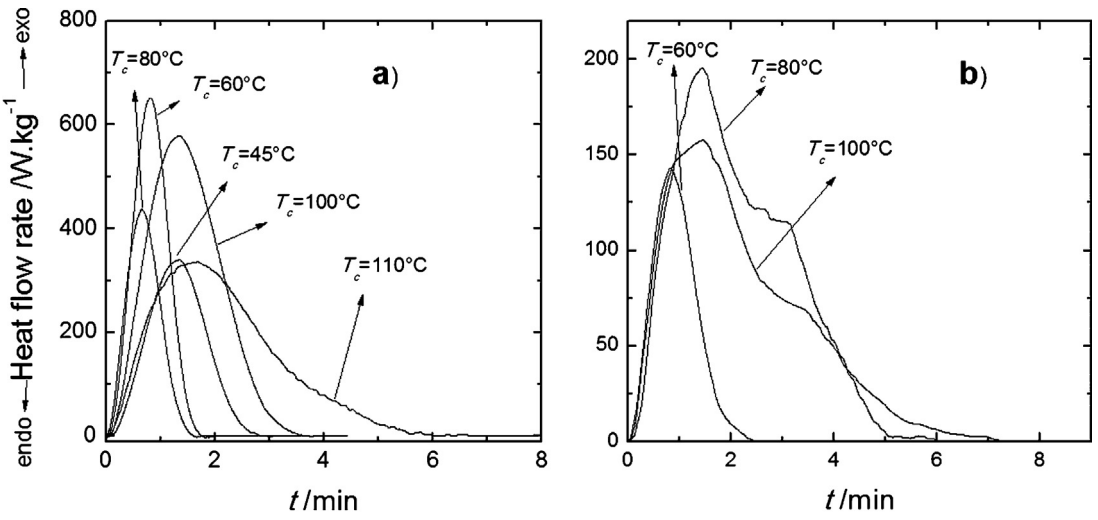

Fig. 4. Thermograms, after background subtraction, for several T_c (see text) for: (a) PHB and (b) PHB/DGEBA 90/10 blend. The curves were horizontally shifted to $t = 0$ for a comparative analysis.

Table 2
n obtained from fitting the thermograms by the Avrami equation for PHB and blends at several crystallization temperatures.

Sample	T_c (°C)	*n*	*n* mean
PHB	45	2.6	2.5
	60	2.9	
	80	2.4	
	100	2.3	
	110	2.2	
PHB/DGEBA 90/10	60	2.6	2.3
	80	2.2	
	100	2.0	
PHB/DGEBA 80/20	45	1.9	2.1
	60	1.9	
	80	2.6	
	100	1.9	
PHB/DGEBA 70/30	45	1.8	1.8
	60	2.0	
	80	1.7	

The reasons behind the differences between both parameters can be attributed to the Avrami equation because it considers the entire crystallization in which different processes are developed, such as nucleation, growth and secondary crystallization. In our analysis, the influence of secondary crystallization was partially reduced, fitting only the first part of the curve of heat flow. However, if the secondary crystallization starts at a time near the primary crystallization, this procedure is inefficient. Moreover, the nucleation cannot be differentiated from growth because, in some cases, it is the factor that controls the crystallization rate.

The index *n* obtained from the fitting shows differences for several T_c's and also shows a clear tendency to decrease with increasing DGEBA in the blend. A diminution of the mean of *n* is observed from 2.5 for pure PHB until 1.8 for the blend PHB/DGEBA 70/30. As reported, *n* depends on the type of nucleation and shape of the crystal growth [13]. If the crystal growth is developed in 3 dimensions (spherulites), a value of 3 or 4 is obtained for *n* according to whether the nucleation has a constant number of nuclei or a constant rate of nucleation, respectively. If the crystal growth is developed in 2 dimensions (discs), the value for *n* is 2 or 3, respectively, in the cases of nucleation mentioned above. The mean value obtained in this work of 2.5 agrees with that reported by You et al. and Hay et al. [37,38] for blends with PEO and PVAc. If it is considered that there is spherulitic growth, the value of *n* would indicate a behavior nearer crystallization with a constant number for the nucleus, according to that observed by optical micrography, in which new spherulites were not formed at the induction time. However, in contrast with the mentioned works, *n* varies with the DGEBA content.

3.3. Induction time

The nucleation process was analyzed using the induction time t_0 determined from calorimetric curves. The determination of t_0 was calculated between the time in which the temperature started the stabilization at the crystallization temperature (approximately 10% over the crystallization temperature) and the time at which the crystallization process started (peaks of heat flow versus time). The values obtained are presented in a plot of $\ln(t_0)$ as a function of T_c for the different blends in Fig. 5. A minimum value for pure PHB can be observed at $T_c = 80\,^{\circ}C$. The values of t_0 are in the range reported by Cyras et al. [39] in [P(HB-co-11%HV)], although the experimental procedure was slightly different because in the present work, the whole process of heating and cooling was performed in the calorimeter. For the blends, the position of minimum shifts to lower temperatures and the time induction increases.

To consider the dependence of t_0 on the temperature, in the literature, Eq. (14) was used [39,40]:

$$t_0 = K_0 \exp\left[\frac{E_{tg}}{R\left(T_c - T_g\right)}\right] exp\left(\frac{E_{tm}}{R\left(T_m^0 - T_c\right)}\right) \quad (14)$$

where, E_{tg} and E_{tm} are activation energies that consider the driving forces of nucleation above T_g and below T_m^0 and K_0 is a pre-exponential factor. The dashed lines in Fig. 5 represent Eq. (14) for the different blends studied. The fitting was performed following a proof-and-error method. The values of E_{tm} and E_{tg} used were 4.45 kJ/mol and 2 kJ/mol, respectively, which were near those obtained by Cyras et al. [39]: 5.76 kJ/mol and 1.79 kJ/mol. As a first approach, Eq. (14) was also used to model the blends, observing that E_{tm} decreases to 3.99 kJ/mol, 3.08 kJ/mol and 2.66 kJ/mol and E_{tg} decreases to 1.66 kJ/mol, 1.25 kJ/mol and 1.06 kJ/mol for the blends 90/10, 80/20 and 70/30, respectively. The pre-exponential factor increases with the increasing DGEBA content with the values 0.005 s (PHB), 0.022 s (PHB/DGEBA 90/10), 0.21 s (PHB/DGEBA 80/20) and 0.53 s (PHB/DGEBA 70/30).

The increase of the induction time when the DGEBA amount is increased could be an indication of a diminution of the nucleation process. This reduction could be associated with a reduction in the density of the nucleus of growth. You et al. [37,38] observed a diminution in the density of the nucleus of growth when the PHB

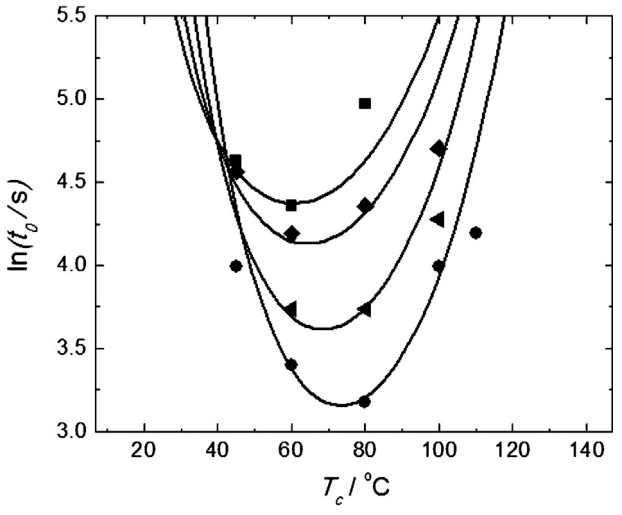

Fig. 5. $\ln(t_0)$ as a function of T_c for PHB (●) and blends with ratios of PHB/DGEBA of 90/10 (◄), 80/20 (♦), and 70/30 (■) (see text). The lines are only a visual guide.

proportion decreased in PHB/PEO blends. In this sense, a combined effect of diminution of nucleation and spherulitic growth may occur when DGEBA is added to PHB.

3.4. Secondary crystallization

Some of the thermograms obtained show a secondary peak located at a time higher than the corresponding to the first peak. This secondary peak was attributed to secondary crystallization. In particular, the secondary peak was clearly observed for PHB crystallized at 110 °C as a broadening of the first peak; PHB/DGEBA 90/10 crystallized at 80 °C and 100 °C (see Fig. 4), and PHB/DGEBA 70/30 crystallized at 45 °C and 60 °C.

A complete analysis of the thermograms considering primary and secondary crystallization is complex because the secondary crystallization depends on the primary crystallization. Several approaches have been used in the literature [41,42]; but in general, numerical evaluations must be performed to fit the experimental results.

From the results obtained, it is feasible to suppose that secondary crystallization is scarce at lower crystallization temperatures. The thermograms corresponding to higher temperatures will be affected by secondary crystallization, and this is reflected in the calculated Avrami index, which decreases from a value of n near 3 for $T_c = 45$ °C and $T_c = 60$ °C to a value of n near 2.3. It is worth mentioning that although the values are lower, Cyras et al. also observed a change of n for temperatures higher than 73 °C with respect to minor temperatures [39]. A temperature of approximately 80 °C would be a limit temperature, which marks off a change in the crystallization process.

4. Conclusions

The crystallization of PHB and PHB/DGEBA blends was studied using optical microscopy and calorimetry. The kinetic of crystallization was analyzed using the theoretical framework of Lauritzen–Hoffman with the usual modifications to consider the non-crystallizable component in the blends. The linear growth rate G of spherulites was determined as a function of the crystallization temperatures. The nucleation constant K_g and the spherulitic growth of the end-surface free energy σ_e were calculated by observing a diminution in σ_e when the DGEBA content increases.

The calorimetric results were described using the Avrami equation. Differences observed in K_g when estimated by calorimetry with respect to the results of optical microscopy were attributed to the fact that the Avrami equation describes only the primary crystallization. Secondary peaks were observed in the calorimetric results and were attributed to secondary crystallization. It was concluded that thermograms corresponding to 80 °C, 100 °C and 110 °C will be affected by secondary crystallization, and this fact affects the Avrami index calculated, which decreases with increasing T_c. The activation energies of the induction process were calculated by observing a diminution with the increase of DGEBA. Changes observed for crystallization temperatures higher than approximately 80 °C with respect to lower temperatures were discussed and are postulated as a possible influence of RAF generation and/or mobilization on the characteristic parameters of the crystallization process.

Acknowledgments

The authors acknowledge the support of *Comisión de Investigaciones Científicas de la Provincia de Buenos Aires*, CIC grant program for projects of scientific and technological research 2013, Res. 813/13, SECAT (UNCPBA), Argentina and ANPCyT-FONCyT, PICT 2013-0686.

References

[1] M. Fujita, T. Sawayanagi, T. Tanaka, T. Iwata, H. Abe, Y. Doi, K. Ito, T. Fujisawa, Synchrotron SAXS and WAXS studies on changes in structural and thermal properties of poly[(R)-3-hydroxybutyrate] single crystals during heating, Macromol. Rapid Commun. 26 (2005) 678–683.
[2] M.C. Righetti, E. Tombari, M.L. Di Lorenzo, The role of the crystallization temperature on the nanophase structure evolution of poly[(R)-3-hydroxybutyrate], J. Phys. Chem. B 117 (2013) 12303–12311.
[3] P. Xing, X. Ai, L. Dong, Z. Feng, Miscibility and crystallization of poly(β-hydroxybutyrate)/poly(vinyl acetate-co-vinyl alcohol) blends, Macromolecules 31 (1998) 6898–6907.
[4] R. Pearce, G.R. Brown, R.H. Marchessault, Crystallization kinetics in blends of isotactic and atactic poly(β-hydroxybutyrate), Polymer 35 (1994) 3894–3989.
[5] M. Avella, E. Martuscelli, Poly-D(-)(3-hydroxybutyrate)/poly(ethylene oxide) blends: phase diagram, thermal and crystallization behaviour, Polymer 29 (1988) 1731–1737.
[6] M.I. Calafel, P.M. Remiro, M.M. Cortázar, M.E. Calahorra, Cold crystallization and multiple melting behavior of poly(L-lactide) in homogeneous and in multiphasic epoxy blends, Colloid. Polym. Sci. 288 (2010) 283–296.
[7] Q. Guo, C. Harrats, G. Groeninckx, H. Reynaers, M.H.J. Koch, Miscibility, crystallization and real-time small-angle X-ray scattering investigation of the semicrystalline morphology in thermosetting polymer blends, Polymer 42 (2001) 6031–6041.
[8] J.D. Hoffman, Regime III crystallization in melt-crystallized polymers: the variable cluster model of chain folding, Polymer 24 (1983) 3–26.
[9] J.I. Lauritzen, J.D. Hoffman, Extension of theory of growth of chain-folded polymer crystals to large undercoolings, J. Appl. Phys. 44 (1973) 4340–4349.
[10] J. Boon, J.M. Azcue, Crystallization kinetics of polymer-diluent mixtures. Influence of benzophenone on the spherulitic growth rate of isotactic polystyrene, J. Polym. Sci. Part A-2 6 (1968) 885–894.
[11] M.L. Di Lorenzo, Spherulite growth rates in binary polymer blends, Prog. Polym. Sci. 28 (2003) 663–689.
[12] G. Groeninckx, M. Vanneste, V. Everaert, Crystallization, morphological structure, and melting of polymer blends, in: L.A. Utraki (Ed.), Polymer Blends Handbook, Kluwer Academic Publishers, Dordrecht, 2002, pp. 203–294.
[13] D. Van Krevelen, K. Nijenhuis, Properties of Polymers, Elsevier, Amsterdam, 2009.
[14] A.T. Lorenzo, M.L. Arnal, J. Albuerne, A.J. Müller, DSC isothermal polymer crystallization kinetics measurements and the use of the Avrami equation to fit the data: guidelines to avoid common problems, Polym. Test. 26 (2007) 222–231.
[15] J. Sĭpusĭć, S. Kurajica, A. Bezjak, Method for induction time determination using data obtained from isothermal crystallization experiment monitored by DSC, J. Appl. Polym. Sci. 93 (2004) 2454–2458.
[16] L. Silva, S. Tognana, W. Salgueiro, Miscibility in crystalline/amorphous blends of poly(3-hydroxybutyrate)/DGEBA, J. Polym. Sci. B: Polym. Phys. 51 (2013) 680–686.
[17] S. Tognana, L. Silva, W. Salgueiro, Crystallization in PHB/DGEBA Blends, J. Polym. Sci. B: Polym. Phys. 52 (2014) 882–886.
[18] S. Tognana, W. Salgueiro, Influence of the rigid amorphous fraction and segregation during crystallization in PHB/DGEBA blends, Polymer Journal, In Press. Available online September 9, 2015. http://www.nature.com/pj/journal/vaop/ncurrent/abs/pj201571a.html.

[19] P.J. Barham, A. Keller, E.L. Otun, P.A. Holmes, Crystallization and morphology of a bacterial thermoplastic: poly-3-hydroxybutyrate, J. Mater. Sci. 19 (1984) 2781–2794.
[20] M.L. Di Lorenzo, E. Raimo, E. Cascone, E. Martuscelli, Poly(3-hydroxybutyrate)-based copolymers and blends: influence of a second component on crystallization and thermal behavior, J. Macromol. Sci: Phys. B40 (2001) 639–667.
[21] S. Cimmino, P. Iodice, E. Martuscelli, C. Silvestre, Poly(3-D(-)hydroxybutyrate)/atactic poly(methylmethacrylate) blends: morphology, miscibility and crystallization relationships, Thermochim. Acta 321 (1998) 89–98.
[22] J.C. Lee, K. Nakajima, T. Ikehara, T. Nishi, Miscibility in blends of poly(3-hydroxybutyrate) and poly(vinylidene chloride-co-acrylonitrile), J. Polym. Sci. B: Polym. Phys. 35 (1997) 2645–2652.
[23] P. Xing, X. Ai, L. Dong, Z. Feng, Miscibility and crystallization of poly(â-hydroxybutyrate)/poly(vinyl acetate-co-vinyl alcohol) blends, Macromolecules 31 (1998) 6898–6907.
[24] J.D. Hoffman, G. Thomas Davis, J.I. Lauritzen Jr., The rate of crystallization of linear polymers with chain folding, in: N.B. Hannay (Ed.), Treatise on Solid State Chemistry, Vol 3, Plenum Press, New York, 1976 (chapter 7).
[25] M.L. Williams, R.F. Landel, J.D. Ferry, The temperature dependence of relaxation mechanisms in amorphous polymers and other glass-forming liquids, J. Am Chem. Soc. 77 (1955) 3701–3707.
[26] Araldite® MY 790 datasheet https://apps.huntsmanservice.com/WebFolder/ui/browse.do?pFileName=/opt/TDS/Huntsman%20Advanced%20Materials/English/Long/Araldite%20MY%20790_eur_e.pdf.
[27] L.L. Zhang, S.H. Goh, S.Y. Lee, G.R. Hee, Miscibility, melting and crystallization behavior of two bacterial polyester/poly(epichlorohydrin-co-ethylene oxide) blend systems, Polymer 41 (2000) 1429–1439.
[28] E. Dubini Paglia, P.L. Beltrame, M. Canetti, A. Seves, E. Martuscelli, Crystallization and thermal behaviour of poly(D(-)3-hydroxybutyrate)/poly(epichlorohydrin) blends, Polymer 34 (1993) 996–1001.
[29] K. Heo, J. Yoon, K.S. Jin, S. Jin, H. Sato, Y. Ozaki, M.M. Satkowski, I. Noda, M. Ree, Structural evolution in microbial polyesters, J. Phys. Chem. B 112 (2008) 4571–4582.
[30] L. Guo, N. Spegazzini, H. Sato, T. Hashimoto, H. Masunaga, S. Sasaki, M. Takata, Y. Ozaki, Multistep crystallization process involving sequential formations of density fluctuations, “intermediate structures”, and lamellar crystallites: poly(3-hydroxybutyrate) as investigated by time-resolved synchrotron SAXS and WAXD, Macromolecules 45 (2012) 313–328.
[31] P.B. Rim, J.P. Runt, Melting point depression in crystalline/compatible polymer blends, Macromolecules 17 (1984) 1520–1526.
[32] M. Pizzoli, M. Scandola, G. Ceccorulli, Crystallization and melting of isotactic poly(3-hydroxy butyrate) in the presence of a low molecular weight diluent, Macromolecules 35 (2002) 3937–3941.
[33] G.C. Alfonso, T.P. Russell, Kinetics of crystallization in semicrystalline/amorphous polymer mixtures, Macromolecules 19 (1986) 1143–1152.
[34] H.D. Keith, F.J. Padden, Spherulitic crystallization from the melt. II. Influence of fractionation and impurity segregation on the kinetics of crystallization, J. Appl. Phys. 35 (1964) 1286–1296.
[35] M. Martínez-Palau, L. Franco, J. Puiggalí, Isothermal crystallization of poly(glycolic acid-alt-6-hydroxyhexanoic acid) studied by DSC and real time synchrotron SAXS/WAXD, Polymer 48 (2007) 6018–6028.
[36] A. Celli, E.D. Zanotto, Polymer crystallization: fold surface free energy determination by different thermal analysis techniques, Thermochim. Acta 269/270 (1995) 191–199.
[37] J.-W. You, H.-J. Chiu, T.-M. Don, Spherulitic morphology and crystallization kinetics of melt-miscible blends of poly(3-hydroxybutyrate) with low molecular weight poly(ethylene oxide), Polymer 44 (2003) 4355–4362.
[38] J.N. Hay, L. Sharma, Crystallisation of poly(3-hydroxybutyrate)/polyvinyl acetate blends, Polymer 41 (2000) 5749–5757.
[39] V.P. Cyras, C. Rozsa, N. Galego, A. Vázquez, Kinetic Expression for the Isothermal Crystallization of Poly(3-hydroxybutyrate)-11%Poly(3-hydroxyvalerate), J. Appl. Polym. Sci. 94 (2004) 1657–1661.
[40] J.M. Kenny, A. Maffezzoli, L. Nicolais, A new kinetic model for polymer crystallization derived by calorimetric analysis, Thermochim. Acta 227 (1993) 83–95.
[41] F.C. Perez-Cardenas, F. Del Castillo, R. Vera-Craziano, Modified Avrami expression for polymer crystallization kinetics, J. Appl. Polym. Sci. 43 (1991) 779–782.
[42] Y.L. Chiari, M. Vadlamudi, R. Chella, K. Jeon, R.G. Alamo, Overall crystallization kinetics of polymorphic propylene-ethylene random copolymers: a two-stage parallel model of Avrami kinetics, Polymer 48 (2007) 3170–3182.